

A STUDY INTO THE FEASIBILITY OF OBTAINING FINITE SOURCE SIZES FROM MACHO-TYPE MICROLENSING LIGHT CURVES

Eric W. Peng

Princeton University Observatory, Princeton, NJ 08544-1001

e-mail: ericpeng@astro.princeton.edu

ABSTRACT

Recent discussion of the effects of finite source size on high magnification microlensing events due to MACHOs motivates a study into the feasibility of observing such effects and extracting the source radius. Simulated observations are generated by adding Gaussian error to points sampled on theoretical microlensing light curves for a limb darkened, extended source. These simulated data sets are fitted in an attempt to see how well the fits extract the radius of the source. The source size can be fitted with reasonable accuracy only if the impact parameter of the event, p , is less than the stellar radius, R_* . It is possible to distinguish “crossing” events, ones where $p < R_*$, from “non-crossing” events if the light curve is well sampled around the peak and photometric error is small — i.e. ≥ 3 observations while the lens transits the disk of the source, and $\sigma_{phot} < 0.08$ mag. These requirements are just within the reach of current observational programs; the use of an early-warning system and multiple observing sites should increase the likelihood that R_* can be fitted. The programs used to simulate and fit data can be obtained via anonymous ftp.

Subject headings: gravitational lenses—microlensing—stars:brown dwarfs

1. INTRODUCTION

Paczynski (1986) noted that if the dark matter constituents of the halo are massive enough, then the optical depth to microlensing is on the order of 10^{-6} . In the past few years, searches for gravitational microlensing events in the LMC and the Galactic Bulge have discovered many plausible candidates through long-term monitoring of millions of stars

(OGLE: Optical Gravitational Lensing Experiment, Udalski et al. 1993; EROS: Experience de Recherche d’Objets Sombres, Aubourg et al. 1993; MACHO: Massive Compact Halo Objects collaboration, Alcock et al. 1993; DUO: Disk Unseen Objects program, Alard et al. 1995). All these projects share the goal of trying to measure the amount of dark matter in the Galactic halo that is in the form of massive compact halo objects (MACHOs).

This study is motivated by recent papers that show the shape of the light curve around the peak to be considerably different from the one predicted for a point source in events where the impact parameter is less than or equal to the source radius. (Witt & Mao 1994; Nemiroff & Wickramasinghe 1994; Gould 1994). The ability to use the light curve of an event to determine the source size, R_*/R_E , where R_E is the Einstein radius, is valuable because we already have an independent estimate of R_* using spectral type. This allows us to use the shape of the light curve to obtain a direct estimate of the value of R_E , which helps to obtain a more accurate estimate of the mass of the lens. The traditional way of estimating R_E requires assumptions of the statistical measures of the relative velocities. Also, knowing the values of R_E and t_0 , the time it takes for the lens to traverse a distance R_E relative to the source in the deflection plane, gives us the transverse velocity.

The approach taken in this paper is limited to single-lens microlensing. Witt (1995) predicts that 3% of microlensing events caused by lenses in the Galactic bulge should show noticeable effect due to the finite source size. Deviations from the point source light curve due to effects such as parallax and binary lenses were ignored for the purposes of this study. Parallax effects have been observed, but occur on time scales much larger than those on which finite source size effects occur (Alcock et al. 1995). Binary lens events, while not insignificant, should only make up $\sim 10\%$ of microlensing candidates toward the Galactic bulge (Mao & Paczyński 1991). However, in the future, the technique used in this study may also be used to investigate these types of deviations.

While it is important to identify the possible effects of finite source size on the light curve, it is equally important to test the feasibility of observing such effects. After a systematic study of generated light curves for single-lens events, this paper determines a lower limit on the sampling rate and photometric accuracy of observations needed to reliably extract R_* from an event. The outline of the paper is as follows: in §2, the general method for generating light curves and the approach to feasibility testing are discussed; in §3, the results are presented and recommendations for observing programs are made.

2. METHOD

The shape of the light curve for a gravitationally lensed extended source can be fully described by five parameters: p , the impact parameter, which is the angular separation between the lens and the unlensed position of the source at the time of maximum magnification (from now on given in units of R_E); R_* , the source radius (also given in units of R_E); t_0 , the time it takes for the lens to traverse a distance R_E relative to the source in the deflection plane; t_{max} , the time of maximum magnification; and mag_0 , the unlensed, or baseline magnitude of the source.

The Einstein ring radius, the distance an image would appear from the line of sight if the lens and source were exactly aligned is given by

$$R_E^2 = \frac{4GMD}{c^2}, \quad D \equiv \frac{D_d(D_s - D_d)}{D_s} \quad (1)$$

where D_d and D_s are the distances to the lens of mass M and to the source, respectively.

The expression for the observed magnitude of a disk of constant surface brightness as a function of position along the trajectory of the lens is derived by Witt & Mao (1994). In this paper, however, all sources are considered to be limb darkened disks with limb darkening parameter 0.6, using the formulation of Aller (1953, p. 207).

When the source and lens move relative to each other in the deflection plane, the magnification varies with time. An example of such a light curve is depicted in Figure 1. Each light curve is labeled with the impact parameter of the source trajectory. Time is given in units of t_0 and R_* for all curves is $0.055 R_E$. Parts of the computer code used to generate these light curves were obtained from Bohdan Paczyński.

The ability to simulate observations not only gives one a large number of sample data sets on which to test potential observational programs, but it also facilitates error analysis by allowing one to compare the values extracted by a fitting routine with the “true” input values. In this model, input parameters were chosen and the theoretical light curve was evenly sampled within each daily observing period, with sampling frequency n . In theory, the length of this daily observing period can range from 1–24 hours. The photometric errors were simulated by adding a random Gaussian error in magnitude to each one of these points. The photometric error for a given observation, σ_{phot} , is a function of magnitude and is given by

$$\sigma_{phot}(mag) = \sigma_0 10^{(mag_0 - mag)/3.5}, \quad \sigma_0 = \sigma_{phot}(mag_0) \quad (2)$$

(Udalski et al. 1994a). Values for σ_0 range from 0.01 mag to 0.25 mag. This dependence was derived from an empirical fit to median OGLE error at different magnitudes. In the future, with better statistics, we will be able to use error histograms to empirically fit the error distribution, and thereby avoid making assumptions of the Gaussian nature of the error.

To test for fitting accuracy, a simulated data set is generated with specific, known parameters. Then, a best-fit microlensing light curve is obtained with a program that uses the Levenberg–Marquardt method for nonlinear fits in multiple dimensions to minimize χ^2 (Press et al. 1992). Figure 2 shows a set of simulated observations and the best-fit light curve. The **rms** photometric error at the baseline magnitude, σ_0 , was taken to be 0.1 mag.

Many different data sets were created and fitted with the goal of investigating error in the extracted source radius as a function of p , σ_0 , n , and the length of the daily observing period. There are a large number of plausible lensing configurations and it would be extremely time-consuming and computer-intensive to examine them all. It was the goal of this study to examine a few extreme cases and a few pertinent ones so that trends in error would be evident, and so that rough, conservative guidelines could be suggested for observing programs. Those interested in testing different cases can access via anonymous **ftp** the original C code used to simulate and fit observations at `astro.princeton.edu`. After login change directory to `bp/finite`. The `read.me` file contains the information about all other files, their names and sizes.

3. RESULTS AND DISCUSSION

In the following discussion, the quantity $R_{\star,fit}$ is used to describe the fitted value for R_{\star} ; the value p_{fit} describes the fitted value for p . Figure 3a plots the percent error in $R_{\star,fit}$ against p_{fit} . Every point represents the fit to simulated observations of an event with random p . The fitted value of the impact parameter is plotted on the x-axis (as opposed to p) because that is what is measured in real data sets. Each extracted value of R_{\star} has an error ($R_{\star,fit} - R_{\star}$). With the exception of p , all the input parameters are identical for every data set. These input values are: $M_{lens} = 0.1 M_{\odot}$, $D_d = 8$ kpc, $D_s = 9$ kpc, $mag_0 = 17.0$ mag, $R_{\star} = 10 R_{\odot}$, $V = 100 \text{ km s}^{-1}$, $n = 2$, $\sigma_0 = 0.0222$ mag, and 24-hour coverage is assumed.

These values give a t_0 of roughly 15 days, an $R_{\star} \sim 0.055 R_E$, and represent a plausible lensing geometry if one is looking toward the Galactic Bulge. This particular lensing configuration was chosen to illustrate the results determined from this study. Events simulated had source radii that ranged from 0.01–1 R_E , and t_0 that ranged from 1–30 days.

The value for the baseline photometric error, σ_0 , in this and all simulations done in this study, was taken from an analysis of OGLE photometry by Udalski et al. (1994). The points represented by “x’s” are “crossing” event simulations, ones where $p < R_{\star}$ and

the lens actually crosses the stellar disk. Circles signify “non–crossing” event simulations, ones where $p > R_\star$, with the radius of each circle proportional to $p - R_\star$. Witt & Mao (1994) have shown that very little differentiates light curves for point source microlensing and extended source microlensing if the impact parameter is larger than the source radius. Error plots, such as Figure 3a, confirm that it is difficult to extract the source radius from a light curve if the lens does not cross the disk of the source.

Figure 3a also illustrates how photometric error quickly blurs any information on the source radius when $p > R_\star$. On the other hand, for “crossing” events, fitting is fairly reliable. The question which follows is: for real observations, where we do not know nature’s input values, can we distinguish “crossing” data sets from “non–crossing” ones? The answer to this question is yes, if our observations are accurate enough.

The dashed line in Figure 3a is the line on which $p_{fit} = R_{\star,fit}$. All points to the left of this line represent simulations in which $p_{fit} < R_{\star,fit}$, i.e. apparent crossing events. All points to the right of this line are simulations in which $p_{fit} > R_{\star,fit}$; apparent non–crossing events. If all apparent crossings correspond to true crossings, i.e. all points to the left of the line are “x’s”, then we are able, from the fitted parameters alone, to distinguish true crossings from true non–crossings. Figure 3a shows a scenario in which this is true. Likewise, all apparent non–crossing events (right of line) correspond to true non–crossing events (circles).

Figure 3b displays the linear relationship between Δp , the error in p_{fit} , and ΔR , the error in $R_{\star,fit}$. As in Figure 3a, every point represents simulated observations of an event with a random p and all other input parameters held constant. We would expect errors in $R_{\star,fit}$ and errors in p_{fit} to be coupled because the light curve is most sensitive to both of these parameters around the time of maximum magnification. Hence, the greater the error in the fitted impact parameter, the greater the error in the fitted stellar radius needs to be in order fit the points on the light curve. The slope of this relationship is a function of the photometric errors and the sampling. Larger errors and fewer observations cause the slope to increase. If this “error slope”, $\Delta R_\star / \Delta p$, has a value less than one, i.e. less than that of the dashed line in Figure 3a, then the relation between p and R_\star will be the same for both input and extracted values; meaning that

$$p < R_\star \iff p_{fit} < R_{\star,fit}.$$

As a result, we should be able to distinguish between “crossing” events and “non–crossing” events using just the fitted values.

The error slope depends on many factors. For any given lensing geometry, the most important ones are: the baseline photometric error, σ_0 , and the observational coverage,

determined by both the sampling frequency, n , and the length of the daily observing period.

3.1. Photometric Error

Assuming that there are an adequate number of evenly spaced observations on a light curve, the photometric error is the quantity that defines the error slope. The χ^2 surface as a function of both p and R_\star possesses a valley in which there is a global minimum. The location of this minimum in the valley is very sensitive to errors in photometry; this can cause it to move significantly. Error slopes were determined using least squares fitting in plots like Figure 3b. Only points for which $\Delta R_{\star,fit} > 0$ were fitted. This is because: 1) the fact that $R_{\star,fit}$ cannot be negative skews the slope for points where $\Delta R_{\star,fit} < 0$, and 2) These points will never cross into the $p_{fit} < R_{\star,fit}$ regime, as exhibited by the lower half of Figure 3a. The trend derived from this rough analysis shows that for $\sigma_0 > 0.08$ mag, the error slope is greater than one and grows slowly with increasing σ_0 ; for $\sigma_0 < 0.08$ mag, the error slope decreases rapidly for decreasing σ_0 . The value $\sigma_0 = 0.08$ mag can be used as a rough upper limit on the photometric error.

However, each lensing configuration is different and some may be more tolerant of photometric errors than others. Since σ_0 is the baseline photometric error, and the part of the light curve with which we are concerned is the peak, the error slope will also be a function of lensing amplitude — photometric error decreases as the source brightens. In events where the source radius is large ($R_\star > 0.5 R_E$), the total magnification is significantly lower than for the point source case, and the resulting photometric errors at the peak are relatively large. However, in these events, the effect of the finite disk is so pronounced that overall, it is still possible to obtain a reasonable fit the source radius provided that there are an adequate number of observations during the crossing of the disk by the lens.

3.2. Sampling Frequency

Even with dense sampling, errors in photometry still prevent fitting from being perfect. Sparse coverage of an event can cause a fitting routine to wander aimlessly, not possessing enough information to determine the global minimum. Frequent and evenly spaced measurements around the time of the peak magnification are essential for good convergence of the fitting routine.

Experiments with the fitting of simulated data sets have shown that some lensing configurations will be more forgiving toward sparse sampling than others. The smaller the impact parameter and the larger the source radius in units of R_E , the easier it is to “resolve” the disk. The most important result obtained from these simulations is that regardless of how high the sampling frequency is on other parts of the light curve, there is very little hope of fitting the source radius without at least one observation while the lens is transiting the disk of the source.

A conservative estimate requires at least three observations during the disk crossing in order to have an error slope less than one. The timing of the observations is most important for a good fit. A single observation exactly at the time of maximum magnification will often result in a good extraction of the source radius. In a sense, it is in an effort to obtain this one point that we must take as many observations as possible around the time of maximum. Multiple observations also reduce the effect of photometric errors and increase the certainty of the fit.

3.3. Observational Programs

Since the time it takes for a lens to cross the disk of a source is usually on the order of one day (and that is for $p = 0$), multi-site coverage, while not an absolute necessity, would greatly increase the chances of resolving a stellar disk. If we assume that there are only 8 hours a night during which a group can observe at one site, then the disk crossing of an event with $t_0 \sim 4$ days and $R_\star = 0.05 R_E$ has a window of only 5 hours, and can be missed entirely if timing is less than fortuitous. Moreover, the light curves of short t_0 events are more prone to exhibit effects due to finite source size because they are likely to involve small lensing masses, which implies a small R_E and a large R_\star/R_E . Early-warning systems, like the ones currently used by the MACHO and OGLE groups (Udalski et al. 1994b), allow resources to be concentrated on a single event and will increase the density of photometry around the time of maximum magnification. Multi-site monitoring of microlensing events, with telescopes in Australia, South Africa, and Chile, has already been initiated by the PLANET collaboration (Probing Lensing Anomalies NETwork; Albrow et al. 1995).

To a limited extent, good photometry can compensate for less than ideal observational coverage and vice versa. However, good quality in both respects is needed to increase the chances that observations of the light curve of a “crossing” event will still contain information on the source size. Nemiroff & Wickramasinghe (1994) emphasize the importance of having enough photometry in order to resolve inflection points in the light

curve. However, this demanding criteria need not be met since the source size can be fit directly as a free parameter, a technique which requires a much lower sampling rate.

The error in $R_{\star,fit}$ shows no discernible trend as a function of t_0 , t_{max} , or mag_0 .

Time resolution and coverage are currently the limiting factors in microlensing observations. Photometric errors in OGLE observations are already within the prescribed limits. Present observational programs that are fortunate enough to detect an extremely high magnification event in the early stages will most likely be able to determine whether or not it is a “crossing” event. For shorter t_0 events, the ability to take observations from more than one site coupled with an early-warning system greatly increases the chances of resolving stellar disks.

I am grateful to Bohdan Paczyński for his insightful advice and enthusiastic support. I thank Hans Witt, Ralph Wijers, and Raja Guhathakurta for helpful comments and discussions. I also thank the referee for useful suggestions. Krzysztof Stanek, Guohong Xu, and Rongsheng Xu all provided valuable assistance with logistics.

REFERENCES

Alard, C. 1995, in Proc. IAU Symp. 173 (Eds. C. S. Kochanek, J. N. Hewitt), Kluwer Academic Publishers, p. 215

Albrow, M. et al. 1995, in Proc. IAU Symp. 173 (Eds. C. S. Kochanek, J. N. Hewitt), Kluwer Academic Publishers, p. 227

Alcock, C. A. et al. 1993, *Nature* 365, 621

Alcock, C. A. et al. 1995, *ApJ*, submitted

Aller, L. H. 1953, *Astrophysics. The Atmospheres of the Sun and Stars*, The Ronald Press Co., New York

Aubourg, E. et al. 1993, *Nature*, 365, 623

Gould, A. 1994, *ApJ*, 421, L71

Mao, S., & Paczyński, B. 1991, *ApJ*, 374, L37

Nemiroff, R. J., & Wickramasinghe, W. A. D. T. 1994, *ApJ*, 424, L21

Paczyński, B. 1986, *ApJ*, 304, 1

Udalski, A., Szymański, M., Kałużny, J., Kubiak, M., Krzemieński, W., Mateo, M., Preston, G. W., & Paczyński, B. 1993, *Acta Astron.*, 43, 289

Udalski, A., Szymański, M., Stanek, K. Z., Kałużny, J., Kubiak, M., Mateo, M., Krzemieński, W., Paczyński, B., & Venkat, R. 1994a, *Acta Astron.*, 44, 165

Udalski, A., Szymański, M., Kałużny, J., Kubiak, M., Mateo, M., Krzemieński, W., & Paczyński, B. 1994b, *Acta Astron.*, 44, 227

Witt, H. J., 1995, *ApJ*, 449, 42

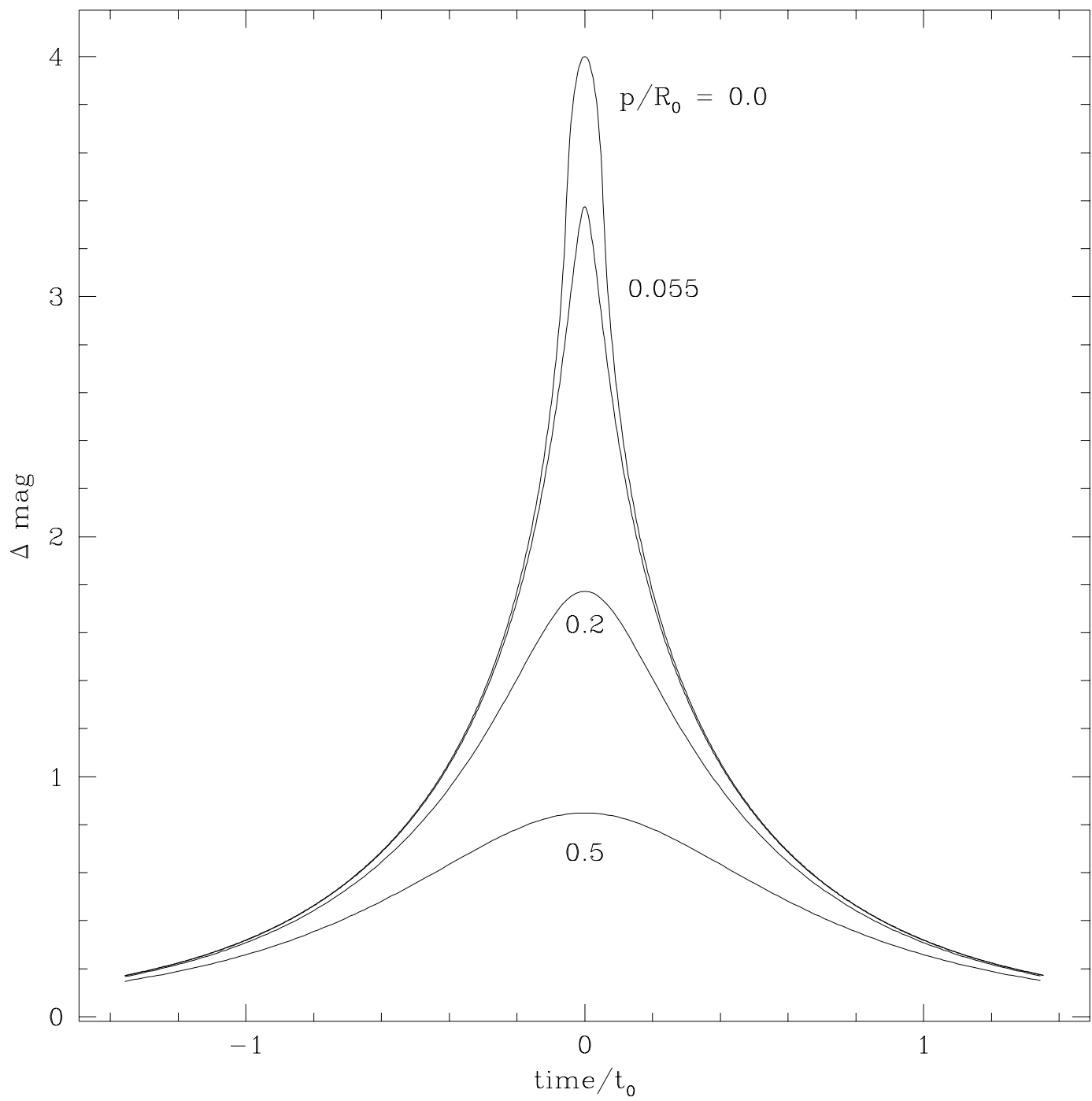
Witt, H. J., & Mao, S. 1994, *ApJ*, 430, 505

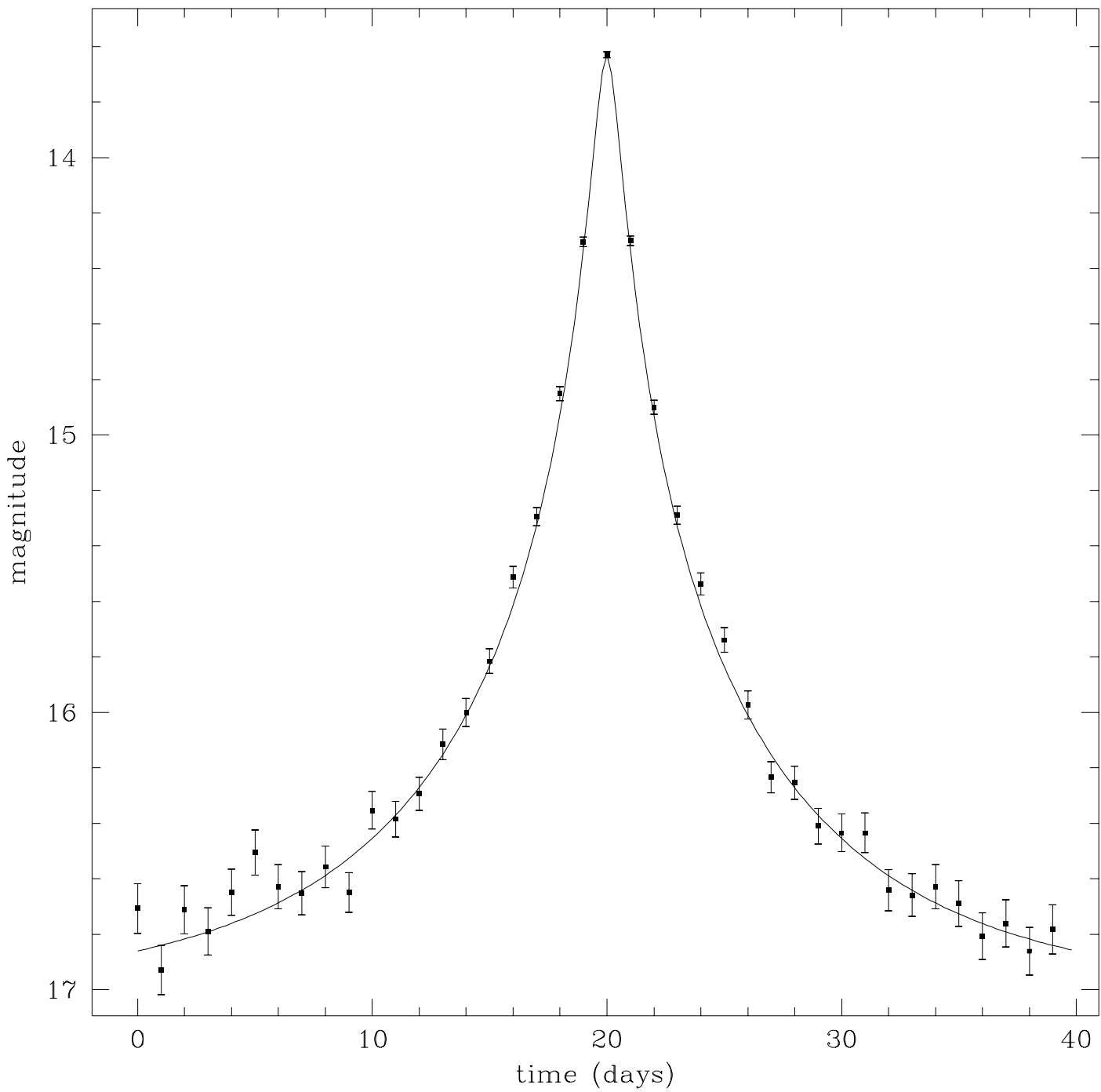
FIGURE CAPTIONS

Fig. 1.— Theoretical light curves for microlensing of an extended, limb darkened source. Shown here are four light curves corresponding to events with impact parameters $p/R_E = 0.0, 0.055, 0.2, 0.5$. The time scale t_0 is defined as the time it takes the lens to move a distance R_E with respect to the source, where R_E is the Einstein ring radius. The other input values for these curves are: $M_{lens} = 0.1M_\odot$, $D_d = 8$ kpc, $D_s = 9$ kpc, $R_\star = 10R_\odot$, $V = 100$ km s $^{-1}$. This gives an $R_\star/R_E = 0.055$. The $p = 0$ event is a “crossing” event; the $p = 0.055$ is an event where the lens grazes the edge of the source; the other two are “non-crossing” events.

Fig. 2.— Simulated observations and the best-fit light curve. These observations were simulated by sampling a theoretical light curve, like the ones shown in Figure 1, and adding a random gaussian error in magnitude. Here, σ_{phot} varies with magnitude with $\sigma_0 = 0.1$ mag. The curve is the best-fit light curve obtained using a Levenberg–Marquardt χ^2 minimization routine. It is useful to compare this best-fit curve to the original theoretical curve to study the errors involved in observation and fitting.

Fig. 3.— a) The percent error in $R_{\star,fit}$ against p_{fit} . Error in the fitted source size is small if $p < R_\star$. When $p > R_\star$, errors rapidly increase. Every point represents a simulated observation for an event with a random p and all other parameters held constant. Points represented by “x’s” are “crossing” event simulations. Circles signify “non-crossing” event simulations with the radius of the circle proportional to $p - R_\star$. In addition to the input parameters used in Figure 1, $mag_0 = 17.0$ mag, $n = 2$, $\sigma_0 = 0.0222$ mag, and 24-hour coverage is assumed. The dashed line is the line on which $p_{fit} = R_{\star,fit}$. All points to the left of this line represent simulations in which $p_{fit} < R_{\star,fit}$, i.e. apparent crossing events. All points to the right of this line are simulations in which $p_{fit} > R_{\star,fit}$; apparent non-crossing events. If all apparent crossings correspond to true crossings, i.e. all points to the left of the line are “x’s”, then we are able, from the fitted parameters alone, to distinguish true crossings from true non-crossings. This figure exhibits a scenario in which this is true. All “crossing” events were fitted with relatively high accuracy. b) The percent error in $R_{\star,fit}$ against the error in p_{fit} , Δp . The relationship between ΔR_\star , $R_{\star,fit} - R_\star$, and Δp is linear for $\Delta R_\star, \Delta p > 0$. The slope of this relationship is a function of the photometric errors and the sampling. Larger errors and fewer observations cause the slope to increase. If this “error slope”, $\Delta R_\star/\Delta p$, has a value less than one, i.e. less than that of the dashed line in Figure 3a, then apparent crossings will correspond to true crossings.





Percent Error: $100 * \Delta R_{\text{star}} / R_{\text{star}}$

